Degenerate Variational Integrators for Magnetic Field Line Flow and Guiding Center Trajectories

C. L. Ellison,[1,2,a] J. M. Finn,[3,b] J. W. Burby,[4] M. Kraus,[5] H. Qin,[2,6] and W. M. Tang[2]
[1] *Lawrence Livermore National Laboratory, Livermore, CA 94550, USA*
[2] *Princeton Plasma Physics Laboratory, Princeton, NJ 08543, USA*
[3] *Los Alamos National Laboratory, Los Alamos, NM 87545, USA*
[4] *Courant Institute of Mathematical Sciences, New York, New York 10012, USA*
[5] *Max-Planck-Institut für Plasmaphysik, Garching, Deutchland*
[6] *Department of Modern Physics, University of Science and Technology of China, Hefei, Anhui 230026, China*

(Dated: 3 April 2018)

Symplectic integrators offer many benefits for numerically approximating solutions to Hamiltonian differential equations, including bounded energy error and the preservation of invariant sets. Two important Hamiltonian systems encountered in plasma physics — the flow of magnetic field lines and the guiding center motion of magnetized charged particles — resist symplectic integration by conventional means because the dynamics are most naturally formulated in non-canonical coordinates. New algorithms were recently developed using the variational integration formalism; however, those integrators were found to admit parasitic mode instabilities due to their multistep character. This work eliminates the multistep character and, therefore, the parasitic mode instabilities via an adaptation of the variational integration formalism that we deem "degenerate variational integration". Both the magnetic field line and guiding center Lagrangians are degenerate in the sense that their resultant Euler-Lagrange equations are systems of first-order ODEs. We show that retaining the same degree of degeneracy when constructing discrete Lagrangians yields one-step variational integrators preserving a non-canonical symplectic structure. Numerical examples demonstrate benefits of the new algorithms, including superior stability relative to existing variational integrators for these systems and superior qualitative behavior relative to non-conservative algorithms.

I. INTRODUCTION

Two of the foundational dynamical systems describing magnetized plasmas, the flow of magnetic field lines and the motion of guiding center trajectories, have long been known to be Hamiltonian[1–3]. The Hamiltonian character of these systems enables the use of powerful analytic tools: the famed KAM theorem bounds the area of stochastic regions in resonantly perturbed tokamaks, for example[4–6]. The Hamiltonian character is equally important for computationally modeling magnetized plasmas: the Liouville theorem is critical for particle-based methods, such as drift- and gyro-kinetic simulations, in which simulated particles advect volume elements of the distribution function, for instance. In general, the numerical integration of Hamiltonian systems has benefitted from a class of methods known as symplectic integrators[7,8]. Symplectic integrators possess an area-preserving property that allows them to retain the Hamiltonian character in numerical trajectories and thereby obtain excellent long term fidelity. They are frequently used to model orbital mechanics and particle accelerators[8,9], for example, and are strong candidates for improved numerical methods in plasma physics[10–16].

Unfortunately, existing symplectic integrators cannot be readily applied to magnetic field line flow or guiding center trajectories. Conventional symplectic integrators are formulated in terms of *canonical* coordinates, that is, coordinates that may be partitioned into positions q and conjugate momenta p whose dynamics are governed by Hamilton's equations in canonical form. Magnetic field line flow and guiding center trajectories are Hamiltonian in a more general sense; the most natural coordinates admit no such partitioning, and are thus deemed *non-canonical*. Although one may transform these systems to canonical coordinates[17–20], at least locally, such transformations either restrict the magnetic geometry or incur a large computational overhead, decreasing the benefits of symplectic integration. The development of symplectic integrators for non-canonical Hamiltonian systems remains an outstanding challenge in numerical analysis[21,22]. In the meantime, magnetized plasma simulations involving the advance of guiding center trajectories resort to non-symplectic algorithms[18,23–27].

Recently, progress toward symplectic integration of guiding center trajectories has been made by applying the theory of variational integration[10,11,28,29]. Instead of applying discrete-time approximations directly to the equations of motion, "variational integrators" (VIs) were constructed by discretizing time in the Lagrangian that underlies the equations of motion by way of a variational principle[30]. By introducing all truncation error into the Lagrangian, the algorithms are guaranteed to preserve *some* symplectic two-form[30]. Although initial results using guiding center VIs exhibited the ex-

[a] Electronic mail: ellison6@llnl.gov
[b] Present address: Tibbar Plasma Technologies, 274 DP Rd, Los Alamos, NM 87544, USA

pected long-term numerical fidelity[10,11,28,29], additional testing revealed numerical instabilities[31,32]. The instabilities were traced[32,33] to the fact that the VIs were *multistep* methods[34–36]; the discrete equations were of higher order than the continuum equations, requiring additional initial conditions, preserving areas in a higher-dimensional phase space, and introducing unphysical "parasitic modes". Before VIs can be considered robust methods for integrating magnetic field line and guiding center equations, these instabilities must be eliminated.

In this contribution, stable VIs are constructed for magnetic field line flow and guiding center trajectories through a novel approach. Specifically, emphasis is placed on retaining the *degeneracy* of the magnetic field line and guiding center Lagrangians when constructing their time-discrete counterparts. These Lagrangians are degenerate in the sense that their corresponding Euler-Lagrange equations are systems of first-order — rather than second-order — ODEs. This is because these Lagrangians are examples of so-called "phase-space Lagrangians"[2,37], Lagrangians whose Euler-Lagrange equations are Hamilton's equations, i.e., a system of first-order ODEs. Conventionally, VIs are assumed to be formed from non-degenerate Lagrangians[30]. The instabilities in previous guiding center VIs may be attributed to the fact that degeneracy was *lost* during the discretization procedure, resulting in a system of second-order difference equations, as would be appropriate for modeling a system of second-order differential equations. By retaining the degeneracy, the VIs obtained here are instead one-step methods, requiring only a single initial condition and preserving non-canonical symplectic structures in the original Hamiltonian phase space. We deem the new integrators "degenerate variational integrators" (DVIs). Although degenerate Lagrangians have been considered in the VI literature[38–40], degeneracy of the discrete Lagrangian was not advocated as desirable until now.

For the magnetic field line DVI, the only restriction used to obtain the desired degree of degeneracy is the choice of an electromagnetic gauge wherein one component of the magnetic vector potential is zero. For the guiding center DVI, one component of the magnetic vector potential is set to zero and it is further assumed that the same covariant component of the magnetic field is zero (in the chosen coordinates). Although many applications of interest do not satisfy this property, this simplification enabled the present progress en route to completing the general problem. In another publication[41], this restriction is avoided through a re-definition of the guiding center coordinates. The new coordinates are chosen to regularize the guiding center equations by eliminating the large-parallel-velocity singularity from the guiding center equations. Simultaneously, the new coordinates enable construction of a guiding center DVI (using the techniques presented in this paper) without any restrictions beyond the existence of a non-vanishing toroidal component of the magnetic field, assumed during the regularizing transformation. For the scope of the present work, we emphasize the DVI technique and restrict attention to the conventional guiding center Lagrangian[1] subject to the aforementioned condition on the coordinates.

The structure of the manuscript is as follows: Section II A introduces degenerate variational integration in the more standard context of canonical Hamiltonian systems. Section II B derives a DVI for non-canonical magnetic field line flow. In Section II C, a guiding center DVI is developed, and the tradeoffs relative to canonical symplectic integration[20] or projected variational integrators[42] are discussed. Section III presents numerical demonstrations, and we conclude in Section IV.

II. DEGENERATE VARIATIONAL INTEGRATORS

A. Canonical Hamiltonian Systems

To (i) demonstrate the need for and (ii) illustrate the development of DVIs, we begin in the context of canonical Hamiltonian systems. Although many techniques are available for deriving symplectic integrators in canonical coordinates[7,9,30,43–46], this subsection introduces the key terminology and methods to be employed in the non-canonical examples of interest. We show that the Leapfrog integrator can be derived as a DVI.

We begin by reviewing the variational formulation of canonical Hamiltonian dynamics. Consider a one-degree-of-freedom (for simplicity) Hamiltonian system described by a coordinate q, conjugate momentum p, and autonomous Hamiltonian $H(q,p)$. The equations of motion may be derived from an action principle employing the following Lagrangian[47,48]:

$$L(q,p,\dot{q},\dot{p}) = p\dot{q} - H(q,p). \tag{1}$$

Because this Lagrangian acts on points (q,p) in the Hamiltonian phase space, it is referred to as a "phase-space Lagrangian"[1,2]. Equation 1 is intimately related to the standard Legendre transform relationship between a Hamiltonian and a Lagrangian:

$$L(q,\dot{q}) = p(q,\dot{q})\dot{q} - H(q,p(q,\dot{q})), \tag{2}$$

where $p(q,\dot{q})$ is a function determined by inverting $\dot{q} = \frac{\partial H}{\partial p}(q,p)$. Note that a phase-space description is retained in Eq. (1) by treating q and p as *independent* coordinates until the Euler-Lagrange equations inform us of their relationship.

To identify Euler-Lagrange equations corresponding to this Lagrangian, consider a path $(q(t),p(t))$ for $t \in [0,T]$ and define an action S acting on the path (q,p) according to

$$S(q,p) = \int_0^T L(q(t),p(t),\dot{q}(t),\dot{p}(t))\ \mathrm{d}t. \tag{3}$$

Hamilton's principle of least action states that the true trajectory extremizes the action functional S. Varying the action with respect to the path (q,p), one obtains

$$\delta S(q,p) = \mathrm{d}S(q,p)\cdot\begin{pmatrix}\delta q\\ \delta p\end{pmatrix} = \int_0^T \Big[\big(\dot{q}(t) - H_{,p}(q(t),p(t))\big)\delta p(t) - \big(\dot{p}(t) + H_{,q}(q(t),p(t))\big)\delta q(t)\Big]\,\mathrm{d}t + p\delta q|_{t=0}^{t=T} \tag{4}$$

where $_{,q}$ denotes differentiation with respect to q, for example, and we have used integration by parts to obtain the result. Asserting that variations at the endpoints are zero[49], the action is extremized by trajectories obeying the following Euler-Lagrange equations:

$$\dot{q} - H_{,p}(q,p) = 0, \tag{5a}$$
$$-\dot{p} - H_{,q}(q,p) = 0, \tag{5b}$$

for all t in $[0,T]$. The canonical phase-space Lagrangian Eq. (1) therefore allows one to derive Hamilton's equations (in canonical coordinates) as the Euler-Lagrange equations of an action principle formulated in phase space[48].

The emergence of a system of first-order ODEs — rather than a system of second-order ODEs — as Euler-Lagrange equations is one indication that the phase-space Lagrangian of Eq. (1) is *degenerate*. To address degeneracy in general, let z represent the generalized coordinates of the Lagrangian, $L(z,\dot{z})$. Here, z is chosen to generalize across the cases of interest for this manuscript; in the canonical setting $z=(q,p)$. A Lagrangian $L(z,\dot{z})$ is defined to be *degenerate* if

$$\det\left(\frac{\partial^2 L}{\partial\dot{z}\partial\dot{z}}\right) = 0. \tag{6}$$

In general, degeneracy is a local property of the Lagrangian, but we will simplify the discussion by assuming the Lagrangian has a globally constant degree of degeneracy (which is true for all Lagrangians considered in this work). To understand the relationship between degeneracy and the order of the Euler-Lagrange system of equations, recall that the Euler-Lagrange equations are in general

$$\frac{\partial L}{\partial z} - \frac{d}{dt}\frac{\partial L}{\partial\dot{z}} = 0, \tag{7}$$

or expanding the time derivative:

$$\frac{\partial L}{\partial z} - \frac{\partial^2 L}{\partial\dot{z}\partial z}\cdot\dot{z} - \frac{\partial^2 L}{\partial\dot{z}\partial\dot{z}}\cdot\ddot{z} = 0. \tag{8}$$

The final term reveals that one is able to uniquely solve for $\ddot{z}(z,\dot{z})$ if and only if the Lagrangian is non-degenerate, or *regular*. If the Hessian matrix $\frac{\partial^2 L}{\partial\dot{z}\partial\dot{z}}$ is not full rank, the order of the Euler-Lagrange ODE system will be reduced. Examining the phase-space Lagrangian Eq. (1), the Hessian $\frac{\partial^2 L}{\partial\dot{z}\partial\dot{z}}$ is completely zero, so no second-order time derivatives appear in Eq. (5) at all. Indeed, the intent of the phase-space Lagrangian is to recover a system of first-order ODEs. Contrast this with a ("configuration-space") Lagrangian of the form:

$$L(q,\dot{q}) = \frac{1}{2}\dot{q}^2 - V(q), \tag{9}$$

which is *not* degenerate and yields a (single) second-order Euler-Lagrange equation.[50]

An important property of Hamiltonian systems is that they preserve a *symplectic structure*[6,51]. In the canonical setting, this means that areas in the (q,p) Hamiltonian phase-space are preserved as they are evolved according to the flow of Hamilton's equations. This property may be rapidly verified using the phase-space action principle and tools from differential geometry; see e.g. Refs. 51 and 52 for accessible introductions to the subject. To show the solutions are symplectic, consider the variation of the action in Eq. (4) *restricted* to act only on trajectories satisfying the Euler-Lagrange equations, Eq. (5). The restricted action $\bar{S}$ can then be considered to be a function of the initial conditions, $(q(0),p(0))$, with the remainder of the path being determined by the solution of the Euler-Lagrange equations. Taking an exterior derivative, the integrand in Eq. (4) is zero, so only the boundary terms from the integration by parts remain:

$$\mathrm{d}\bar{S}(q(0),p(0)) = p(T)\mathrm{d}q(T) - p(0)\mathrm{d}q(0), \tag{10}$$

where again $(q(T),p(T)$ are determined by the initial conditions according to the Euler-Lagrange equations. We then take a second exterior derivative combined with the property that $\mathrm{d}^2=0$ (a differential geometric analog of $\nabla\times\nabla=0$ and $\nabla\cdot\nabla\times=0$) to show

$$\mathrm{d}q\wedge\mathrm{d}p|_{t=0} = \mathrm{d}q\wedge\mathrm{d}p|_{t=T}. \tag{11}$$

That is, the solutions of Hamilton's equations preserve the "differential two-form" $\Omega = \mathrm{d}q\wedge\mathrm{d}p$. This two-form is a twice-covariant anti-symmetric tensor that calculates the area spanned by two vectors in the Hamiltonian phase-space. The fact that solutions to Hamilton's equations preserve this symplectic structure means that as two arbitrary vectors are evolved along the solution to Hamilton's equations, the area they span will remain constant; see Fig. 1.

Turning now to the construction of numerical solutions to Eq. (5), it is desirable to choose a numerical method that also preserves these phase-space areas, i.e., a *symplectic integrator*. Symplectic integrators generate trajectories that are nearby to *some* Hamiltonian system that converges to the original as the step size approaches zero (provided the method is consistent)[7,8]. If the Hamiltonian of the continuous system is $H(q,p)$, then a backward error analysis reveals that the numerical solution after one time step is the time-h solution to a Hamiltonian

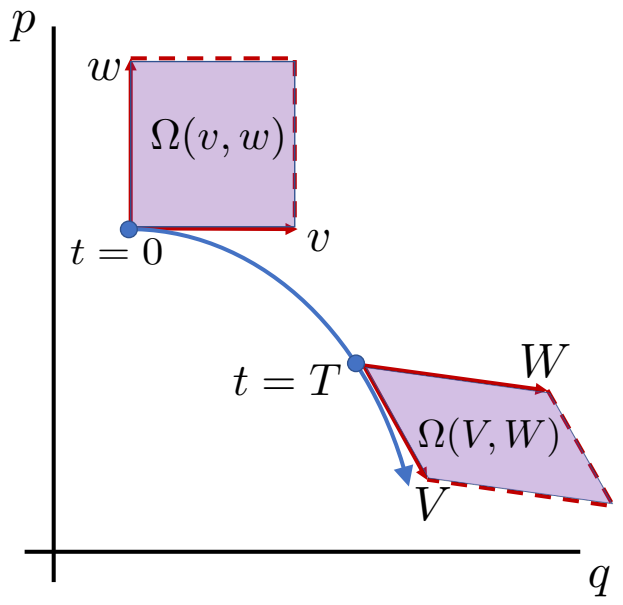

FIG. 1. Canonical Hamiltonian systems preserve phase-space area. Given two vectors (v, w) at some initial point at time $t = 0$, the area they span is given by $\Omega(v, w)$. At a later time $t = T$, the vectors have evolved to (V, W), but the area they span $\Omega(V, W)$ remains constant. Because this is true for any v, w and any time T, this property is referred to as preserving the symplectic structure Ω. In multiple degrees of freedom, the sum of the areas in each of the q^i, p_i planes is preserved. In non-canonical systems, the areas are weighted by non-constant components of Ω.

system of the form:

$$\widetilde{H}(q,p) = H(q,p) + hH_1(q,p) + h^2H_2(q,p) + ..., \quad (12)$$

where the power series in h is asymptotic[7] and the H_i functions depend on H and its derivatives. Although the solution is an approximation of the true dynamics, symplectic integrators ensure that the *character* of the solution remains Hamiltonian. This leads to many desirable properties, including bounded energy errors (for systems with time-independent Hamiltonians), subject to the technical qualifications of the asymptotic expansion above.

One way to systematically construct algorithms that preserve *some* symplectic structure is to use a technique known as variational integration, wherein all discrete-time approximations are introduced to the Lagrangian and the action[30]. The numerical algorithm is determined by requiring the numerical trajectory (a path that is now discrete in time) to extremize the discrete-time action. The determination of a symplectic structure preserved by the VI then follows the same procedure as used to determine Eq. (11).

As an illustration of this variational integration procedure, and an example of what can go wrong in the context of degenerate Lagrangian systems, consider the following "midpoint discrete Lagrangian":

$$L_d(z_k, z_{k+1}) = \frac{p_k + p_{k+1}}{2}\frac{q_{k+1} - q_k}{h} - \frac{1}{2}\left(H(q_k, p_k) + H(q_{k+1}, p_{k+1})\right), \quad (13)$$

where $z = (q, p)^T$, z_k denotes the numerical solution at time t_k and the timestep is h. The *discrete action* S_d corresponding to this discrete Lagrangian is a summation over the time interval:

$$S_d(z_0, z_1, ..., z_N) = \sum_{k=0}^{N-1} hL_d(z_k, z_{k+1}), \quad (14)$$

where the time interval $[0, T]$ has been divided into N increments of equal size h. This summation is clearly a discretized version of the integral in Eq. (3). A discrete analog of the Euler-Lagrange equations, dubbed the *discrete Euler-Lagrange equations*, is obtained by requiring the discrete action to be stationary with respect to variations in z_k for all $k = 1, ..., N - 1$, so

$$\delta S_d = h\sum_{k=1}^{N-1}\left(\frac{\partial L_d(z_{k-1}, z_k)}{\partial z_k} + \frac{\partial L_d(z_k, z_{k+1})}{\partial z_k}\right)\cdot\delta z_k + h\frac{\partial L_d(z_0, z_1)}{\partial z_0}\cdot\delta z_0 + h\frac{\partial L_d(z_{N-1}, z_N)}{\partial z_N}\cdot\delta z_N. \quad (15)$$

Again asserting the variations are zero at the endpoints, the discrete action is extremized by discrete trajectories satisfying the discrete *Euler-Lagrange equations*:

$$\frac{\partial L_d(z_{k-1}, z_k)}{\partial z_k} + \frac{\partial L_d(z_k, z_{k+1})}{\partial z_k} = 0, \quad (16)$$

for all $k = 1, ..., N - 1$. For the midpoint discrete Lagrangian in Eq. (13), the discrete Euler-Lagrange equations are:

$$-p_{k+1} + p_{k-1} - 2hH_{,q}(q_k, p_k) = 0, \quad (17a)$$
$$q_{k+1} - q_{k-1} - 2hH_{,p}(q_k, p_k) = 0. \quad (17b)$$

Immediately, we observe that something went awry during the discretization procedure. Whereas the continuous equations of motion, Eq. (5), are a system of first-order differential equations, the discrete Euler-Lagrange equations above manifest a system of *second-order* difference schemes: to determine (q_{k+1}, p_{k+1}), one must supply both (q_{k-1}, p_{k-1}) and (q_k, p_k). Because of this discrepancy between the order of the continuous and discrete equations, Eq. (17) is referred to as a *multistep method*[35,36]; it is a two-step method for solving a system of first-order differential equations. This is not to be confused with *multistage* methods, such as Runge-Kutta schemes, which evaluate the ODE vector field at multiple intermediate stages of a timestep but do not require additional initial conditions. The particular multistep scheme

obtained above is referred to as the "explicit midpoint scheme"[36].

Because the explicit midpoint scheme is a higher-order difference system than the continuous equations it models, the numerical trajectory it generates contains additional modes not present in the continuum dynamics. These additional "parasitic" modes[36,53] have deleterious effects on the conservation and stability properties of the VI. Beginning with the conservation properties, the motivation for deriving an integrator from a discrete variational principle is to obtain an area-preserving result analogous to that of Eq. (11)[30]. To calculate the symplectic structure preserved by the explicit midpoint scheme, one restricts Eq. (15) to act on trajectories satisfying the discrete Euler Lagrange equations, then takes a second exterior derivative to identify a differential two-form preserved by the numerical solution. The result is

$$\mathrm{d}q_1 \wedge \mathrm{d}p_0 + \mathrm{d}q_0 \wedge \mathrm{d}p_1 = \mathrm{d}q_{N-1} \wedge \mathrm{d}p_N + \mathrm{d}q_N \wedge \mathrm{d}p_{N-1}. \quad (18)$$

Although this symplectic two-form resembles that of the continuous system ($\mathrm{d}q \wedge \mathrm{d}p$), it resides on a space *twice* as large as the original Hamiltonian phase space! The two-form in Eq. (11) and Fig. 1 is on a two-dimensional space (with coordinates (q,p)), whereas this two-form is on a four-dimensional space (with coordinates (q_0,p_0,q_1,p_1)). Because the multistep VI preserves areas in a higher dimensional space, we cannot expect it to behave the same as familiar symplectic integrators; that is, we cannot expect the numerical trajectory to be a solution to a Hamiltonian system of the form of Eq. (12).

In addition to preserving the wrong symplectic structure, the multistep character of the explicit midpoint algorithm introduces numerical instabilities. We demonstrate these instabilities by applying the algorithm to the nonlinear pendulum system, $H(q,p) = p^2/2 + 1 - \cos(q)$; the results are shown in Fig. 2. To highlight the presence of the spurious numerical mode, the even- and odd-numbered steps are distinguished with white and black markers, respectively. At early times, the trajectory appears to be smooth and a good representation of the physical dynamics. As time progresses, however, the presence of unphysical modes becomes apparent as the even- and odd-indexed trajectories diverge. The even-odd character arises because the parasitic modes correspond to eigenvalues near negative one in a linear stability analysis. The presence of such a numerical instability in Fig. 2 indicates that the four-dimensional symplectic structure in Eq. (18) is insufficient for obtaining the desired long-term numerical fidelity. Moreover, it has been recently shown that *any* variationally-derived multistep method cannot have parasitic modes that are all damped[33]; if one parasitic mode is damped, there exists another parasitic mode that is unstable and amplified in time. The best prospect is to eliminate the parasitic modes altogether.

Interestingly, it is not especially difficult to select a discretization of the canonical phase-space Lagrangian that eliminates the parasitic modes. Instead of choosing the

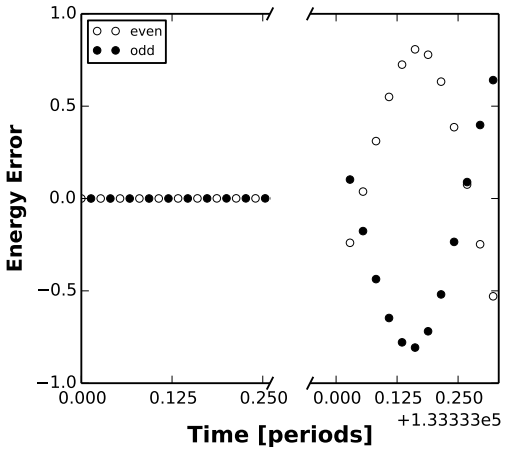

FIG. 2. The two-step VI, Eq. (17), admits parasitic mode instabilities when applied to the nonlinear pendulum problem. At early times, the even- and odd-indexed points in the trajectory lie on a smooth curve. After $\approx 10^5$ oscillation periods, a large even-odd oscillation distorts the trajectory, as evidenced by the order-unity energy error. Initial condition: $(q,p) = (1,0)$; timestep $h = 0.1$.

midpoint discretization of Eq. (13), consider the following discretization:

$$L_d(q_k,p_k,q_{k+1},p_{k+1}) = p_k \frac{q_{k+1}-q_k}{h} - H(q_{k+1},p_k). \quad (19)$$

The discrete Euler-Lagrange equations for this system are given by

$$p_k - p_{k+1} - hH_{,q}(q_{k+1},p_k) = 0, \quad (20a)$$
$$q_{k+1} - q_k - hH_{,p}(q_{k+1},p_k) = 0. \quad (20b)$$

In contrast to the first VI, this algorithm is a one-step method, requiring only a single initial condition (q_0,p_0). No parasitic modes can possibly be present because the order of the difference equations matches the order of the ODE system. This VI is also well known as the symplectic Euler scheme[54]. For separable Hamiltonian systems, i.e., Hamiltonians of the form $H(q,p) = K(p) + V(q)$, this is the same as a Leapfrog scheme if one instead interprets the momentum coordinates as "staggered": $p_k \mapsto p_{k+1/2}$. This VI may be shown to be symplectic by again appealing to the variational principle. Restricting the discrete action to act on trajectories satisfying the discrete Euler-Lagrange equations (20), the first exterior derivative of the restricted discrete action gives

$$\mathrm{d}\bar{S}_d(q_0,p_0) = -p_0\mathrm{d}q_0 + p_N\mathrm{d}q_N. \quad (21)$$

Taking a second exterior derivative recovers the desired result:

$$\mathrm{d}q_0 \wedge \mathrm{d}p_0 = \mathrm{d}q_N \wedge \mathrm{d}p_N. \quad (22)$$

This VI therefore preserves the *same* symplectic two-form as the true Hamiltonian system; both the symplectic

Euler scheme and the Leapfrog advance are well known to be symplectic.

Although the parasitic modes have been eliminated, the preceding VI is not centered in time and is only first-order accurate. It is of course desirable to achieve second-order accuracy, which could be approached in a number of ways. Choosing a time-centered discrete Lagrangian apparently introduces parasitic mode instabilities, as shown with the explicit midpoint method. An alternative route to time symmetrization is to alternate the time advance between a first-order scheme and its *adjoint*. The adjoint scheme results from transforming $h \mapsto -h$ and swapping k and $k+1$ in the discrete Lagrangian[30]:

$$L_d(q_k, p_k, q_{k+1}, p_{k+1}) = p_{k+1}\frac{q_{k+1}-q_k}{h} - H(q_k, p_{k+1}). \tag{23}$$

The resulting VI will be the other symplectic Euler scheme — the adjoint of the previous method, involving implicit determination of p_{k+1} followed by explicit identification of q_{k+1}[55]. By alternating between the two symplectic Euler schemes, the composition is time symmetric and therefore second-order accurate. For this system, both of the symplectic Euler integrators used in the composition preserve the same (canonical) symplectic structure, so their composition also preserves the canonical symplectic structure and therefore exhibits the expected long-term numerical fidelity. Later we will encounter DVIs that preserve *different* symplectic structures than their adjoint, so the conservation properties of the accuracy-enhancing composition will be less clear.

The most important lesson from these examples is that simply changing the choice of discrete Lagrangian recovered a system of first-order difference schemes, thereby eliminating the parasitic mode instabilities and preserving a symplectic two-form on the Hamiltonian phase space. The question inspired by these studies becomes: *which* discrete Lagrangians will yield one-step methods? This question has been addressed in detail in a recent doctoral thesis[33], and in brief may be explained as a result of degeneracy in the *discrete* Lagrangian. To examine degeneracy in the discrete setting, let us return to generalized coordinates z representing the arguments of the Lagrangian. A discrete Lagrangian typically depends on z_k and z_{k+1}, so $L_d = L_d(z_k, z_{k+1})$. The discrete Lagrangian is defined to be *degenerate* if[30]

$$\det\left(\frac{\partial^2 L_d}{\partial z_k \partial z_{k+1}}\right) = 0. \tag{24}$$

Just like the continuous degeneracy condition, the degeneracy condition for a discrete Lagrangian may be understood as a solvability condition for the discrete Euler-Lagrange equations, Eq. (16). According to the implicit function theorem, a necessary and sufficient condition for solving for z_{k+1} as a function of (z_k, z_{k-1}) is that the discrete Lagrangian is non-degenerate. That is, the discrete Euler-Lagrange equations are a well-defined system of second-order difference schemes if and only if the discrete Lagrangian is non-degenerate.

The experiment yielding the symplectic Euler/Leapfrog scheme illustrates that — much like the phase-space Lagrangian — degeneracy of the discrete Lagrangian can correspond to a *reduction* in the *order* of the resulting system of difference equations. In fact, the discrete degeneracy condition in Eq. (24) serves as a useful guide for discerning which Lagrangians will yield a multistep method from those that yield a reduced order system of difference equations. For example, the midpoint discrete Lagrangian Eq. (13) is *not* degenerate:

$$\frac{\partial^2 L_d(z_k, z_{k+1})}{\partial z_k \partial z_{k+1}} = \begin{pmatrix} 0 & \frac{-1}{2h} \\ \frac{1}{2h} & 0 \end{pmatrix}, \tag{25}$$

ensuring a system of second-order difference equations (Eq. (17)), which exceeds the order of the original differential equations (Eq. (5)). In contrast, the discrete Lagrangian in Eq. (19), which yielded the symplectic Euler/Leapfrog advance, *is* degenerate:

$$\frac{\partial^2 L_d(z_k, z_{k+1})}{\partial z_k \partial z_{k+1}} = \begin{pmatrix} 0 & 0 \\ \frac{1}{h} - H_{,pq}(q_{k+1}, p_k) & 0 \end{pmatrix}, \tag{26}$$

so the rank is one and the determinant is zero. This degeneracy indicates that the discrete Euler-Lagrange equations cannot be a system of second-order difference equations; instead, we identified a one-step method in Eq. (20).

In general, matching the order of the difference equations to the order of the differential equations requires the two systems to be degenerate to "the same degree". It is not sufficient to simply ensure that both the continuous and discrete Lagrangians are degenerate, but rather one must ensure the orders of the relevant systems of equations are the same. Let us then call a discrete Lagrangian that is degenerate and whose discrete Euler-Lagrange equations have the same order as the continuous system *properly degenerate*.

The condition for an arbitrary discrete Lagrangian to be properly degenerate is discussed in general in a recent thesis[33]. For the scope of this manuscript, we claim without proof that a discrete Lagrangian is properly degenerate if the rank of the Hessian tensor referred to in Eq. (24) equals the number of degrees of freedom. In lieu of proving this order matching condition, we will show case-by-case that the presented integrators satisfy the condition, are one-step methods, and preserve symplectic structures on the Hamiltonian phase space. Note that it is not yet known how to systematically construct VIs satisfying the proper degeneracy condition, but the condition remains useful nonetheless for rapidly assessing whether a chosen discrete Lagrangian will yield a one-step method.

The ensuing subsections build upon the intuition established above, striving to develop VIs with the proper degree of degeneracy for magnetic field line flow and guiding center trajectories. These two Hamiltonian systems also stem from phase-space Lagrangians, albeit in forms

more general than the canonical phase-space Lagrangian. To see how these more general *non-canonical* phase-space Lagrangians might come about, consider an arbitrary coordinate transformation of the form

$$(q,p) \mapsto z(q,p).$$

In this case, the phase-space Lagrangian becomes

$$\begin{aligned} L(z,\dot{z}) &= p(z)\cdot\frac{\partial q}{\partial z}\cdot\dot{z} - H(z) \\ &= \vartheta(z)\cdot\dot{z} - H(z). \end{aligned} \tag{27}$$

Both the magnetic field line and guiding center Lagrangians are in the form of Eq. (27). Indeed, such a "non-canonical coordinate transformation" plays a central role in the derivation of Hamiltonian guiding center dynamics[1,3]. Deriving DVIs from the non-canonical phase-space Lagrangian introduces challenges not encountered in the canonical setting.

B. Magnetic Field Line DVI

Consider a time-independent magnetic vector potential $A(x)$ and a corresponding magnetic field $B = \nabla\times A$. (For time-dependent fields, field lines are traced at a single, fixed instant in time.) One can trace or "follow" magnetic field lines by solving the differential equation

$$\frac{dx}{d\tau} = B(x), \tag{28}$$

where τ parameterizes the distance along the field line from some initial location x_0.

To reveal the underlying Hamiltonian character of this problem[2], *choose* one of the spatial coordinates — say x^3 — to be the independent parameter. That is, we seek determination of the field line trajectory as given by the functions $x^1(x^3), x^2(x^3)$. In this parameterization, the "magnetic field line Lagrangian" is given by[2]:

$$L(x^1,x^2,\dot{x}^1,\dot{x}^2,x^3) = A_1\dot{x}^1 + A_2\dot{x}^2 + A_3, \tag{29}$$

where the "dot" now denotes the derivative with respect to x^3. This Lagrangian has the form of a non-canonical phase-space Lagrangian, i.e. an instance of Eq. (27) where $z = (x^1,x^2)$, $t = x^3$, $\vartheta = (A_1,A_2)$, and $H(z,t) = -A_3(x^1,x^2,x^3)$. The Euler-Lagrange equations for this phase-space Lagrangian give the non-canonical Hamilton's equations[2]:

$$\dot{x}^1 = \frac{B^1}{B^3}, \tag{30a}$$

$$\dot{x}^2 = \frac{B^2}{B^3}. \tag{30b}$$

Like all phase-space Lagrangians, the magnetic field line Lagrangian Eq. (29) is degenerate as defined in Eq. (6).

The action principle may be used to show that this non-canonical Hamiltonian system preserves a non-canonical symplectic structure:

$$\Omega = (A_{1,2}(x) - A_{2,1}(x))\,\mathrm{d}x^1\wedge\mathrm{d}x^2. \tag{31}$$

The physical interpretation of this property is that the B^3 magnetic flux will be preserved as areas are evolved along with the flow of the Hamiltonian system. Whereas canonical Hamiltonian systems preserve area in the (q,p)-plane, magnetic field line flow preserves the B^3 flux in the (x^1,x^2)-plane.

To construct a one-step VI for this system, a properly degenerate discretization needs to be chosen for the magnetic field line Lagrangian Eq. (29). Building upon the intuition developed in the canonical section, a reasonable first guess for a discretization that might yield a one-step method would be

$$\begin{aligned} L_d(x_k,x_{k+1}) =& A_1(x_{k+1})\frac{x^1_{k+1}-x^1_k}{h} + \\ & A_2(x_{k+1})\frac{x^2_{k+1}-x^2_k}{h} + A_3(x_{k+1}). \end{aligned} \tag{32}$$

However, this does not yield a one-step method or a DVI for a general magnetic vector potential A. Checking the degeneracy condition for a discrete Lagrangian (see Eq. (24)),

$$\frac{\partial^2 L_d}{\partial z_k \partial z_{k+1}} = \frac{-1}{h}\begin{pmatrix} A_{1,1}(x_{k+1}) & A_{1,2}(x_{k+1}) \\ A_{2,1}(x_{k+1}) & A_{2,2}(x_{k+1}) \end{pmatrix}, \tag{33}$$

which is a full-rank, non-degenerate tensor for general A. If the discrete Lagrangian is not degenerate, then the VI must be a two-step method and parasitic modes will be present. It is a straightforward exercise to calculate the discrete Euler-Lagrange equations for this discrete Lagrangian and indeed find a system of second-order difference equations.

The form of Eq. (33), however, motivates the introduction of the desired degeneracy using an electromagnetic gauge transformation. If we choose an electromagnetic gauge such that, e.g.,

$$A_1 = 0, \tag{34}$$

then the discrete Lagrangian in Eq. (32) reduces to

$$L_d(x_k,x_{k+1}) = A_2(x_{k+1})\frac{x^2_{k+1}-x^2_k}{h} + A_3(x_{k+1}), \tag{35}$$

which *is* degenerate:

$$\frac{\partial^2 L_d}{\partial z_k \partial z_{k+1}} = \frac{-1}{h}\begin{pmatrix} 0 & 0 \\ A_{2,1}(x_{k+1}) & A_{2,2}(x_{k+1}) \end{pmatrix}, \tag{36}$$

with rank one. In Sec. II A, we claimed that if the rank of this tensor matches the number of degrees of freedom then the VI will be a one-step method. To find such a

one-step DVI in this case, begin by varying the discrete action:

$$\delta S_d = \sum_{k=1}^{N-1} \Big[\big(A_{2,1}(x_k)(x_k^2 - x_{k-1}^2) + hA_{3,1}(x_k)\big)\,\delta x_k^1 + \big(A_{2,2}(x_k)(x_k^2 - x_{k-1}^2) - A_2(x_{k+1}) + A_2(x_k) + hA_{3,2}(x_k)\big)\delta x_k^2 \Big] - A_2(x_1)\delta x_0^2 + A_2(x_{N+1})\delta x_N^2. \quad (37)$$

With zero variations at the endpoints, the discrete action is extremized by the following discrete Euler-Lagrange equations:

$$A_{2,1}(x_k)\left(x_k^2 - x_{k-1}^2\right) + hA_{3,1}(x_k) = 0, \quad (38a)$$

$$A_{2,2}(x_k)\left(x_k^2 - x_{k-1}^2\right) + A_2(x_k) - A_2(x_{k+1}) + hA_{3,2}(x_k) = 0, \quad (38b)$$

for $k = 1, ..., N$. Here we notice an interesting distinction from the symplectic Euler discrete Euler-Lagrange equations in Eq. (20): the first of these equations contains evaluations at time t_{k-1}, t_k, *and* t_{k+1}, giving the appearance of a multistep method. Guided by the degeneracy condition, however, we are confident that a reduction in order has taken place. In fact, one can formulate a one-step method from the above equations as follows: (i) Use Eq. (38a) to *determine* x_{k-1}^2 as a function of x_k (ii) Replace x_{k-1}^2 in Eq. (38b) with this relation and (iii) write Eq. (38a) at one time index later. The result is

$$A_{2,1}(x_{k+1})\left(x_{k+1}^2 - x_k^2\right) + hA_{3,1}(x_{k+1}) = 0, \quad (39a)$$

$$-hA_{2,2}(x_k)\left(\frac{A_{3,1}(x_k)}{A_{2,1}(x_k)}\right) + A_2(x_k) - A_2(x_{k+1}) + hA_{3,2}(x_{k+1}) = 0. \quad (39b)$$

That is, we have obtained a one-step VI for magnetic field line flow in the $A_1 = 0$ gauge. This update is valid provided $A_{2,1} \neq 0$, which implies B^3 is non-zero, as previously assumed. Note that this one-step formulation generates trajectories that satisfy Eq. (38); we have merely re-arranged the equation into a one-step method.

It is interesting to note that one cannot express Eq. (39) as a direct differencing of the equations of motion Eq. (30). In particular, the VI requires evaluations of the magnetic vector potential A, for example in the term $A_2(x_k)$, meaning the integrator is not gauge invariant (*even* among gauges satisfying $A_1 = 0$). By Taylor expanding $A_2(x_{k+1}) - A_2(x_k)$, the gauge-dependent terms appear in the $\mathcal{O}(h^2)$ truncation error for this first-order method, and therefore any gauge-dependent effects will diminish as the numerical step size approaches zero. Although it is not necessarily desirable to require specification of a magnetic vector potential when numerically tracing field lines, such a gauge dependence is common among VIs for field-particle systems[10–12,31].

The symplectic structure preserved by this VI may be calculated from the boundary terms in the discrete variational principle. Restricting attention to trajectories satisfying the discrete Euler-Lagrange equations, Eq. (39), the derivative of the restricted action is

$$\mathrm{d}\bar{S}_d(x_0) = A_2(x_{N+1})\mathrm{d}x_N^2 - A_2(x_1)\mathrm{d}x_0^2, \quad (40)$$

where we recall that x_1 is a function of x_0 according to the one-step discrete Euler-Lagrange equations, Eq. (39), so $x_1 = F(x_0)$ and x_{N+1} actually denotes $F^{N+1}(x_0)$. Taking a second exterior derivative and $d^2 S_d = 0$ then obtains:

$$\mathrm{d}(A_2(F(x_0))\mathrm{d}x_0^2) = \mathrm{d}(A_2(F(x_N))\mathrm{d}x_N^2), \quad (41)$$

so F preserves a symplectic structure Ω_d given by:

$$\Omega_d = -\left(A_{2,1}(F(x))\frac{\partial F^1}{\partial x^1} + A_{2,2}(F(x))\frac{\partial F^2}{\partial x^1}\right)\mathrm{d}x^1 \wedge \mathrm{d}x^2. \quad (42)$$

Comparing with Eq. (31), we see that the discrete symplectic structure Ω_d is not exactly the same as the continuous symplectic structure Ω. They do agree, however, in the $h \to 0$ limit: as the numerical step size h tends to zero, F becomes the identity map, so $\frac{\partial F^2}{\partial x^1} = 0$ and $\frac{\partial F^1}{\partial x^1} = 1$, and of course $A_1 = 0$. In this sense, the discrete symplectic structure Ω_d may be considered to be nearby Ω for small h. Whereas the continuous magnetic field line flow preserves magnetic flux in the (x^1, x^2)-plane, the DVI preserves something closely related to the magnetic flux in the same (x^1, x^2)-plane.

The DVI in Eq. (39) is first-order accurate; in order to recover a degenerate discrete Lagrangian, we did not choose a time-symmetric discretization. After obtaining the one-step method, it is desirable to increase its order of accuracy to second-order. One approach would be to compose the DVI with its adjoint scheme, which can be derived by interchanging k and $k+1$ in the discrete Lagrangian and mapping $h \mapsto -h$. The adjoint discrete Lagrangian to Eq. (35) is then

$$L_d(x_k, x_{k+1}) = A_2(x_k)\frac{x_{k+1}^2 - x_k^2}{h} + A_3(x_k), \quad (43)$$

where the $A_1 = 0$ gauge is still assumed. The corresponding discrete Euler-Lagrange equations are the adjoint (c.f. the discussion surrounding Eq. (23)) of the previous magnetic field DVI, Eq. (39). If we label the time advance of the DVI in Eq. (39) as F and its adjoint $F^\dagger$, then a second-order accurate method will be given by $F^\dagger \circ F$. An important question, however, is what symplectic structure, is preserved by the new, time-symmetric scheme.

Typically, symplectic integrators preserve the *same* symplectic structure as that of the continuous dynamics. In that case, the integrator and its adjoint both preserve the same symplectic structure and their composition is also symplectic, preserving the symplectic structure of the continuous system. Here, the symplectic structure preserved by $F^\dagger$ is

$$\left(A_{2,2}(F^\dagger(x))\frac{\partial (F^\dagger)^2}{\partial x^1} - A_{2,1}(F^\dagger(x))\frac{\partial (F^\dagger)^1}{\partial x^1}\right)\mathrm{d}x^1 \wedge \mathrm{d}x^2. \quad (44)$$

i.e., it is *not* the same as the symplectic structure preserved by F, but also approaches Ω as h tends to zero. It is then unclear what symplectic structure, if any, might be preserved by the composition of the two maps. To ensure the conservation properties remain intact, it may be preferable to apply an accuracy-enhancing processing technique[56,57] instead of the aforementioned composition scheme.

C. Guiding Center DVI

The final application is the ubiquitous guiding center system. Littlejohn derived the following guiding center Lagrangian[1]:

$$L(x,u,\dot{x},\dot{u}) = (A(x)+ub(x))\cdot\dot{x} - H_{gc}(x,u), \qquad (45)$$

where $u=\dot{x}\cdot b$ is the parallel velocity, b is the magnetic field unit vector, and H_{gc} is the guiding center Hamiltonian,

$$H_{gc}(x,u) = \frac{1}{2}u^2 + \mu\|B\|(x) + \phi(x), \qquad (46)$$

where μ is the (constant) magnetic moment of the particle and $\|B\|$ is the magnitude of the magnetic field. In both of these definitions, the fields have been assumed to be time independent for simplicity. Also, the vector potential A has been normalized by $\frac{e}{mc}$ and the electrostatic potential ϕ has been normalized by $\frac{e}{m}$, where e is the charge of the particle of interest, m its mass, and c the speed of light. This Lagrangian is in the form of a non-canonical phase-space Lagrangian, Eq. (27), with $z=(x,u)$ and $\vartheta=(A+ub,0)$.

The Euler-Lagrange equations corresponding to the guiding center Lagrangian describe the cross-field drifts and along-field motion while preserving the Hamiltonian character of the original full-orbit description. Letting $A^\dagger = A+ub$ and using index notation with Einstein summation, the guiding center Euler-Lagrange equations are

$$\left(A^\dagger_{i,j} - A^\dagger_{j,i}\right)\dot{x}^i - b_j\dot{u} - \mu\|B\|_{,j} - \phi_{,j} = 0, \quad j=1,2,3 \qquad (47a)$$

$$b_i\dot{x}^i - u = 0, \qquad (47b)$$

where indices appearing after a comma denote differentiation with respect to the corresponding coordinate. These equations contain: parallel motion along the magnetic field, the $E\times B$ drift, the ∇B drift, and the curvature drift. The polarization drift (relevant when time-dependent fields are considered) may be incorporated by including $E\times B$ velocity contributions in the definition of guiding center Lagrangian[3].

As can be shown from the action principle in phase space, guiding center trajectories preserve the following symplectic structure:

$$\Omega_{gc} = A^\dagger_{i,j}(z)\mathrm{d}z^j\wedge\mathrm{d}x^i, \qquad (48)$$

with $i=1,2,3$ and $j=(1,2,3,4)$ to account for $z=(x,u)$. Whereas canonical Hamiltonian systems preserve areas in the (p,q) phase-space plane and magnetic field lines preserve magnetic flux through the (x^1,x^2) phase-space plane, guiding center trajectories preserve flux of the *effective magnetic field* $B^\dagger=\nabla\times A^\dagger$ through the (x^i,x^j)-position coordinate planes, plus areas in the (u,x^i) planes weighted by the i^{th} component of the magnetic field unit vector.

This four-dimensional Hamiltonian system in non-canonical coordinates (x,u) comes about by performing non-canonical coordinate transformations to the charged particle phase-space Lagrangian[1]. Early attempts at formulating the guiding center equations based on the drift dynamics alone[58] yielded non-Hamiltonian systems. Littlejohn's seminal work on Hamiltonian guiding center theory attacked the problem by (i) beginning with the canonical phase-space Lagrangian for a particle under the influence of the Lorentz force, (ii) performing non-canonical coordinate transformations to identify the ignorable gyrophase θ and the adiabatically invariant magnetic moment μ as two of the six phase-space coordinates and (iii) truncating the guiding center Lagrangian by retaining only first-order terms in the guiding center expansion[1]. Obtaining the ignorable θ and constant μ as non-canonical coordinates enabled the reduction of dimensionality from the six-dimensional full-orbit phase space to the four-dimensional (two degree-of-freedom) guiding center phase space. Meanwhile, performing all approximations upon the phase-space Lagrangian rather than the equations of motion preserved the Hamiltonian character of the system. An interesting point in the context of this work is that the degeneracy of the Lagrangian is introduced in step (i) as a means of enabling transformations on all six phase-space coordinates; the gyroaveraging/dynamical reduction does not introduce any additional degeneracy, but instead simply lowers the dimensionality of the dynamics while making it difficult to return to canonical coordinates.

Turning now to the construction of a DVI for Eq. (47), two assumptions will be made: First, one covariant component of the magnetic vector potential A_i will be chosen to be zero using the electromagnetic gauge freedom, as in Sec. II B. Second, the *same covariant* component of the magnetic field unit vector b_i will be assumed to be zero so that one component of $A^\dagger$ is eliminated altogether. This condition is satisfiable, at least with local coordinates; for instance, several of the procedures for constructing canonical coordinates for the guiding center system achieve this property as an intermediate step[18–20]. Note however that we will *not* transform to canonical coordinates when deriving this integrator. Note also that this assumption has been relaxed in another work that builds upon the formalism employed here[41].

Proceeding with the assumption that, e.g., the first component of both A and b are zero yields a guiding center Lagrangian of the form

$$L(z,\dot{z}) = A^\dagger_2(z)\dot{x}^2 + A^\dagger_3(z)\dot{x}^3 - H_{gc}(z), \qquad (49)$$

where $z = (x, u)^T$.

In direct analogy with the discrete Lagrangian for the magnetic field line DVI, Eq. (35), let us choose the following discrete Lagrangian for the guiding center dynamics:

$$\begin{aligned} L_d(z_k, z_{k+1}) &= L_{GC}(z_{k+1}, \frac{z_{k+1} - z_k}{h}) \\ &= A^\dagger(z_{k+1}) \cdot \frac{x_{k+1} - x_k}{h} - H_{gc}(z_{k+1}). \end{aligned} \quad (50)$$

Minimizing the discrete action yields the following discrete Euler-Lagrange equations:

$$\begin{aligned} \nabla A^\dagger(z_k) \cdot (x_k - x_{k-1}) - A^\dagger(z_{k+1}) + A^\dagger(z_k) - \\ h \nabla H_{gc}(z_k) = 0, \quad (51a) \\ \nabla_u A^\dagger(z_k) \cdot (x_k - x_{k-1}) - h \nabla_u H_{gc}(z_k) = 0. \quad (51b) \end{aligned}$$

As in Section II B, it appears at first glance as if a multistep scheme has been obtained; the discrete Euler-Lagrange equations include variables evaluated at times t_{k-1}, t_k, t_{k+1}. The Hessian informs us, however, that the chosen discrete Lagrangian is indeed properly degenerate:

$$\frac{\partial^2 L_d(z_k, z_{k+1})}{\partial z_k \partial z_{k+1}} = \begin{pmatrix} 0 & 0 & 0 & 0 \\ A^\dagger_{2,1} & A^\dagger_{2,2} & A^\dagger_{2,3} & 0 \\ A^\dagger_{3,1} & A^\dagger_{3,2} & A^\dagger_{3,3} & 0 \\ 0 & 0 & 0 & 0 \end{pmatrix}, \quad (52)$$

where all evaluations in the final term are at z_{k+1}. The Hessian therefore has rank two, which is equal to the number of degrees-of-freedom of the guiding center system indicating the chosen discrete Lagrangian is properly degenerate. Because the discrete Lagrangian is degenerate, the discrete Euler-Lagrange equations in Eq. (51) cannot specify a two-step method; because it is properly degenerate, we claim (and proceed to demonstrate) that it is a one-step method. At this point, the necessity of the condition on A and b is apparent: if they did not share a non-zero component, then the Hessian would have non-zero terms in the top row and would not have rank two. Furthermore, because $A^\dagger$ has only two non-zero components, variables at time t_{k+1} only appear in two components of Eq. (51), which will allow us to reformulate the equations as a one-step method. As in Section II B, this reformulation proceeds by: (i) advancing any equations lacking a z_{k+1} forward in time one index and (ii) replacing $x_k^2 - x_{k-1}^2$ and $x_k^3 - x_{k-1}^3$ in the apparently three-step equations as functions of variables at time t_k. The resulting one-step formulation of Eq. (51) is

$$\begin{aligned} A^\dagger_{2,1}(z_{k+1})(x^2_{k+1} - x^2_k) + A^\dagger_{3,1}(z_{k+1})(x^3_{k+1} - x^3_k) - h(\mu B_{,1}(x_{k+1}) + \phi_{,1}(x_{k+1})) = 0, \\ A^\dagger_{2,2}(z_k)\Delta^2 + A^\dagger_{3,2}(z_k)\Delta^3 - (A^\dagger_2(z_{k+1}) - A^\dagger_2(z_k)) - h(\mu B_{,2}(x_k) + \phi_{,2}(x_k)) = 0, \\ A^\dagger_{2,3}(z_k)\Delta^2 + A^\dagger_{3,3}(z_k)\Delta^3 - (A^\dagger_3(z_{k+1}) - A^\dagger_3(z_k)) - h(\mu B_{,3}(x_k) + \phi_{,3}(x_k)) = 0, \\ b_2(x_{k+1})(x^2_{k+1} - x^2_k) + b_3(x_{k+1})(x^3_{k+1} - x^3_k) - h u_{k+1} = 0, \end{aligned} \quad (53)$$

where, according to Eq. (51), Δ is given by

$$\begin{pmatrix} A^\dagger_{2,1} & A^\dagger_{3,1} \\ b_2 & b_3 \end{pmatrix} \begin{pmatrix} \Delta^2 \\ \Delta^3 \end{pmatrix} = h \begin{pmatrix} \mu B_{,1} + \phi_{,1} \\ u_k \end{pmatrix}, \quad (54)$$

where all fields are evaluated at (z_k).

Being variational in nature, the guiding center DVI preserves a symplectic two-form. Restricting the discrete action to act only on trajectories generated by the one-step DVI, the derivative of the restricted discrete action is

$$\mathrm{d}\bar{S}_d(z_0) = -A^\dagger_i(z_1)\mathrm{d}x^i_0 - A^\dagger_i(z_{N+1})\mathrm{d}x^i_N, \quad (55)$$

where, letting F denote the one-step DVI advance (as in Eq.(41)), $z_k = F^k(z_0)$. This equation is analogous to Eq. (40) for the magnetic field line problem and Eq. (21) for canonical systems. Taking a second exterior derivative identifies the symplectic structure preserved by the DVI to be

$$\Omega_d = A^\dagger_{i,j}(F(z))\frac{\partial F^j}{\partial z^k}\mathrm{d}z^k \wedge \mathrm{d}x^i, \quad (56)$$

which is analogous to Eq. (42) in the magnetic field line problem. This symplectic two-form approaches the guiding center symplectic two-form, Eq. (48), in the zero step-size limit. As $h \to 0$, F approaches the identity map, so the symplectic two-form becomes:

$$\lim_{h\to 0} \Omega_d = A^\dagger_{i,j}(x_0)\mathrm{d}z^j_0 \wedge \mathrm{d}x^i_0, \quad (57)$$

i.e. $\lim_{h\to 0} \Omega_d = \Omega_{gc}$.

Like the magnetic field line DVI, a natural improvement to the guiding center DVI would be to obtain second-order accuracy in time. Care must be taken to retain the desired stability and conservation properties. Previous guiding center VIs used time-centered discrete Lagrangians to achieve second-order accuracy[10,11,28,29].

However, none of these methods were properly degenerate, so they were multistep and unstable[32,33]. As discussed in Sections II B and II A, second-order accuracy can also be achieved by composing the DVI with its adjoint, formed by interchanging $z_k \leftrightarrow z_{k+1}$ and mapping $h \mapsto -h$ in the discrete Lagrangian. However, the adjoint guiding center DVI does not preserve the same symplectic structure as the presented DVI (as was the case for the magnetic field line DVI). Because it is then unclear what symplectic structure might be preserved by the composition of these two methods, it may be preferable to instead use an accuracy-enhancing processing technique[56,57] rather than a time symmetrization approach; for now, this remains as future work.

Of course, one way to achieve higher-order accuracy would be to use canonical guiding center coordinates[19,20]; many high-order canonical symplectic integration schemes are known[7,9,59]. In fact, it is trivial to identify canonical coordinates for the guiding center Lagrangian after assuming $A_1 = b_1 = 0$. Choosing

$$p_2 = A_2^\dagger, \tag{58a}$$

$$p_3 = A_3^\dagger, \tag{58b}$$

Eq. (49) becomes:

$$\begin{aligned} &L(x^2, x^3, p_2, p_3, \dot{x}^2, \dot{x}^3, \dot{p}_2, \dot{p}_3) = \\ &\quad p_2\dot{x}^2 + p_3\dot{x}^3 - H_{gc}(x^2, x^3, p_2, p_3), \end{aligned} \tag{59}$$

i.e., a canonical phase-space Lagrangian. The disadvantage to this approach is that the Hamiltonian is typically known as a function of (x^1, x^2, x^3, u) without an explicit representation in the canonical coordinates. Although the transformation *to* canonical coordinates is explicit, the inverse transformation to the non-canonical coordinates (in which the field functions are typically defined) requires an iterative scheme. These iterations incur computational expense. The DVI algorithm in non-canonical coordinates avoids these iterations and therefore has the prospect of being advantageous relative to canonical symplectic integration.

A similar comparison can be made with the "projected variational integrators" developed in Ref. 42. Projected variational integrators address the problem of variational integration of phase-space Lagrangians by formulating the problem as a high dimensional canonical Hamiltonian system subject to constraints. For guiding center dynamics, the 4-D non-canonical system can be represented as an 8-D canonical system subject to (four) algebraic constraints. The projections ensure the numerical trajectory satisfies the same constraints as those governing the continuous system, and are effective for achieving good long-term behavior[42]. Although a variational formulation for the post-projected dynamics has not been found, it has been shown to be symplectic[42]. Advantages of projected variational integrators include their applicability to any (non-canonical) phase-space Lagrangian and their higher-order accuracy, including second- and fourth-order accuracy. The disadvantage relative to degenerate variational integration is the introduction of additional variables in the nonlinear solve, making them less efficient in this sense.

III. NUMERICAL DEMONSTRATIONS

In this section, we demonstrate the long-term fidelity achieved by DVIs through their variational, structure preserving formulation. The instabilities inherent to previous VIs for these systems are shown to be eliminated. The benefits of the conservation properties are illustrated by showing that the DVIs capture the correct qualitative behavior of the Hamiltonian dynamics; a feature that is lost by non-conservative schemes even if they have high-order local accuracy.

The numerical examples in this section utilize tokamak magnetic geometry represented in toroidal coordinates (r, θ, ϕ), where r is the minor-radial position, θ the geometric poloidal angle, and ϕ the geometric toroidal angle. Two magnetic fields are considered: the axisymmetric magnetic field used in Ref. 11, and the same field with an added resonant magnetic perturbation. The axisymmetric magnetic field is given by[11]

$$B(r, \theta, \phi) = \frac{B_0}{q_0(R_0 + r\cos\theta)} e_\theta + \frac{B_0 R_0}{(R_0 + r\cos\theta)^2} e_\phi, \tag{60}$$

where B_0 is the on-axis magnetic field magnitude, q_0 the on-axis safety factor, R_0 the major radius and e_θ, e_ϕ are basis elements for contravariant vectors in toroidal coordinates (i.e., e_θ, e_ϕ are not unit vectors). This axisymmetric magnetic field may be derived from the magnetic vector potential

$$\begin{aligned} &A(r, \theta, \phi) = \\ &B_0 R_0 \left(\frac{r}{\cos\theta} - \frac{R_0 \log\left(1 + \frac{r\cos\theta}{R_0}\right)}{\cos^2\theta} \right) \nabla\theta - \frac{B_0 r^2}{2q_0} \nabla\phi. \end{aligned} \tag{61}$$

Note that $A_r = 0$, as posited in the development of the magnetic field line and guiding center VIs. It is also the case that $b_r = 0$ for these axisymmetric fields, so the guiding center DVI can be constructed in the (r, θ, ϕ) coordinates.

The second magnetic configuration applies resonant perturbations to the first vector potential:

$$\tilde{A}(r, \theta, \phi) = A(r, \theta, \phi) - \frac{B_0 r^2}{2q_0} \sum_i \delta_i \sin(m_i\theta - n_i\phi) \nabla\phi, \tag{62}$$

where $A(r, \theta, \phi)$ is given by Eq. (61), and δ_i is the size of the i'th perturbation with mode numbers m_i and n_i. This perturbation in the toroidal component of A incurs perturbations in the radial and poloidal components of the otherwise axisymmetric magnetic field in Eq. (60).

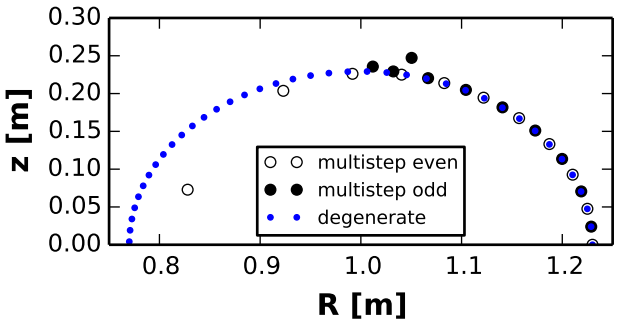

FIG. 3. The multistep VI exhibits parasitic mode instabilities when used to trace magnetic field lines, wheres the DVI generates a smooth trajectory. Here we show the (R, z) projection of successive steps in the trajectory, where $R = R_0 + r$.

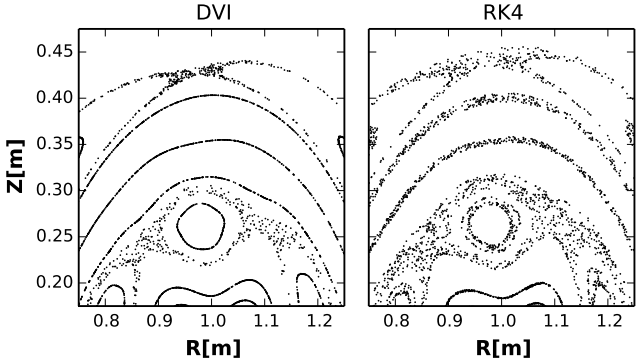

FIG. 4. The magnetic field line DVI correctly distinguishes between integrable and stochastic trajectories in the resonantly perturbed tokamak, whereas the non-conservative RK4 algorithm blurs the distinction. Figure reproduced with permission from the author's dissertation[33].

A. Magnetic Field Line Flow

First, the importance of proper degeneracy is emphasized by tracing field lines in the axisymmetric configuration using the DVI in Eq. (39) and a non-degenerate (i.e., multistep) variational integrator defined by the discrete Lagrangian in Eq. (32) *without* one component of the magnetic vector potential being zero. For this latter VI, we use the following magnetic vector potential:

$$\bar{A} = \bar{A}_r \nabla r + \frac{A_\theta}{2} \nabla\theta + A_\phi \nabla\phi \tag{63a}$$

$$\bar{A}_r = -\frac{B_0 R_0 r}{\sqrt{R_0^2 - r^2}} \arctan\left(\frac{(R_0 - r)\tan(\theta/2)}{\sqrt{R_0^2 - r^2}} \right), \tag{63b}$$

where A_θ, A_ϕ are defined according to Eq. (61). This is simply a gauge transformation of the original vector potential, intended to violate the condition that one component of the potential be zero. In these studies, we use $B_0 = 1\text{T}$, $R_0 = 100\text{cm}$, and $q_0 = \sqrt{2}$.

In Fig. 3, a field line is traced using the DVI and the non-degenerate, multistep VI. The trajectory generated by the multistep VI is highly unstable; parasitic mode oscillations cause the even- and odd-indexed steps in the trajectory to diverge after just a few steps. Meanwhile, the DVI exhibits no such instability by virtue of being a one-step method.

The next demonstration verifies that the DVI captures the Hamiltonian nature of the magnetic field line equations. In particular, we simulate a resonantly perturbed tokamak with two Fourier components: an $(m_1 = 3, n_1 = 2)$ harmonic and an $(m_2 = 7, n_2 = 5)$ harmonic, both with amplitude $\delta_i = 3.5 \times 10^{-4}$, for $i = 1, 2$. Several field lines are initialized beginning at different radii. A Poincaré section is then formed by intersecting the trajectory with a plane of constant toroidal angle ϕ. Both integrations use a step size of $h = 0.5$ and advance for 3×10^6 steps. The results for the DVI may be found in the left panel of Fig. 4 and contrasted with the results of a fourth-order Runge-Kutta simulation on the right.

The salient difference between the two algorithms is that the DVI readily distinguishes between *integrable* and *stochastic* trajectories. Integrable trajectories correspond to those that reside on a magnetic flux surface, generating one-dimensional curves in the Poincaré surface of section. Meanwhile, stochastic trajectories arise near separatrices and fill two-dimensional areas in the Poincaré section. Of course, in the axisymmetric, $\delta_i \to 0$ limit, all magnetic field lines reside on flux surfaces. As small, symmetry-breaking perturbations are introduced, narrow stochastic regions emerge near trajectories that resonate with the perturbation. It is a Hamiltonian property, explained by the KAM theorem, that these regions should be bounded by magnetic flux surfaces for sufficiently small perturbations. This fundamentally Hamiltonian behavior is readily identifiable in the trajectory calculated using the DVI. On the other hand, although the fourth-order Runge-Kutta (RK4) scheme exhibits much less local error, all of the trajectories appear area-filling in the Poincaré section over long integrations. Note that the numerical step size was chosen to be small enough to avoid introducing numerically induced stochasticity[60]; the DVI portrait appears similar even at smaller step sizes.

To best illustrate the qualitative distinctions between the algorithms, this comparison was performed at equal numerical step size. Note, however, that the implicit DVI is several times more computationally expensive, per step, than the explicit RK4 scheme. An equal computational expense comparison, allowing RK4 to execute more steps of smaller size, would eventually reveal the same qualitative behavior but requires much longer simulations.

B. Guiding Center Trajectories

The non-canonical guiding center system bears many similarities to the non-canonical magnetic field line system. Here we show that the benefits demonstrated in the magnetic field line context carry over to the guiding center system.

Preceding this work, guiding center VIs have been multistep methods[10,11,28,29]. In certain configurations, the parasitic modes inherent to these methods can become unstable, leading to even-odd oscillations akin to those observed in Figs. 2 and 3. As an example of this behavior in the guiding center context, we first produce a guiding center trapped-particle "banana orbit" trajectory using the VI developed in Ref. 28, which uses the discrete Lagrangian

$$L_d(x_k, x_{k+1}, u_{k+1/2}) = A^\dagger(\frac{x_k + x_{k+1}}{2}, u_{k+1/2}) \cdot \frac{x_{k+1} - x_k}{h} - hH_{gc}(\frac{x_k + x_{k+1}}{2}, u_{k+1/2}). \tag{64}$$

Here, the parallel velocity coordinate u has been "staggered" in time with respect to the position coordinates. The staggering of this coordinate is made possible by the absence of its time derivative, $\dot{u}$, in the Lagrangian. The motivation for such a staggering was to enhance the stability of the algorithm[28], which we now understand to be related to the parasitic mode oscillations. Indeed, the algorithm was believed to be stable when first presented; the parasitic modes are difficult to detect for many configurations, depending on the electric and magnetic fields, the particle's initial condition, and the numerical step size. As evidenced by the left panel of Fig. 5, however, parasitic modes remain present in this VI. The figure depicts a trapped particle "banana-orbit" trajectory in the axisymmetric magnetic field in Eq. (60) with $B_0 = 1$ T, $R_0 = 100$ cm, $q_0 = \sqrt{2}$ and with initial condition $(r, \theta, \phi, u, \mu) = (5, 0, 0, -0.129, 2.1 \times 10^{-4})$ in the normalized units. The numerical step size corresponds to roughly 600 steps per bounce period. At early times, the even- and odd-indexed steps form a smooth trajectory in the R, z-plane. These are the central points in the inset zoom. As time progresses, however, the even- and odd-indexed trajectories diverge, leading to the leftmost white and rightmost black markers, respectively. Soon after the depicted time, the nonlinear solve fails to converge due to the large amplitude of the parasitic mode oscillation.

Interestingly, the staggering of the parallel velocity in this scheme introduces some of the desirable degeneracy into the discrete Lagrangian, albeit not enough to obtain a one-step method and eliminate all of the parasitic modes. The integrator specifies an update from $(x_{k-1}, u_{k-1/2}, x_k)$ to $(u_{k+1/2}, x_{k+1})$, so two position initial conditions are required but only one parallel velocity initial condition is required. From the perspective of a degeneracy calculation, this manifests as the Hessian matrix for the discrete Lagrangian in Eq. (64) having rank three. Although it is degenerate (full rank would be four), it is not *properly degenerate*, which would be rank two for the guiding center system.

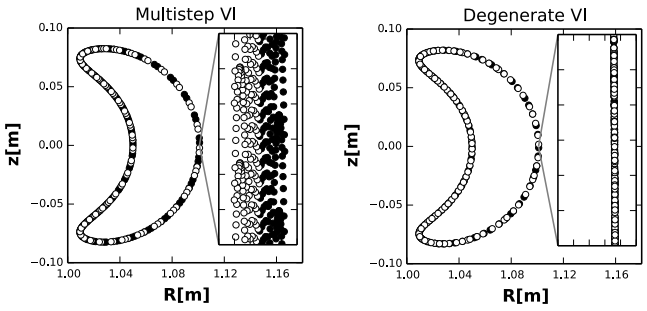

FIG. 5. The guiding center DVI successfully eliminates the parasitic mode instabilities present in existing variational guiding center algorithms. Even-indexed points are marked in white, and odd-indexed points in black. These trapped particle trajectories were evolved in the axisymmetric magnetic field given in Eq. (60). The insets have a width of 10^{-4} m in the R-direction and 3×10^{-4} m in the z-direction. Although the parasitic mode oscillations appear small, they cause the Newton-Rhapson iterations to fail to converge, crashing the simulation. Figure reproduced with permission from the author's dissertation[33].

In the right panel of Fig. 5, we evolve the trapped particle trajectory using the DVI derived in Section II C. The smooth trajectory is evidence that the parasitic modes have been completely eliminated. The proper degeneracy of the DVI led to a one-step method, so no parasitic modes can be present in this scheme.

Now that the stability of the guiding center DVI has been established, we examine its long-term behavior. In Fig. 6, a passing particle trajectory is advanced using the DVI algorithm and RK4. Parameters for this study were chosen to correspond to a 3.5 MeV alpha particle in an ITER-like configuration. In the normalized units, the field parameters are given by: $B_0 = 255.6$, $R_0 = 6.20$, $q_0 = \sqrt{2}$ and initial condition $(r, \theta, \phi, u, \mu) = (0.31, 0, 0, -5.2, 0.277)$[61]. Equal numerical step sizes were used for the two algorithms with 25 steps per orbit period (a complete revolution in the $R - z$ plane).

Although the RK4 algorithm introduces much less error on any given step, the errors accumulate in qualitatively different manner. The energy error for RK4 is unbounded; meanwhile, the energy error for the DVI algorithm remains bounded by a few percent. Such behavior is indicative of the DVI preserving *some* energy function that differs from the true energy in a stepsize-dependent way (c.f. Eq. (12)). The differences between the schemes are also apparent in the evolution of the trajectory in the $R - z$ plane: the DVI maintains a closed trajectory, whereas RK4 exhibits an increasingly distorted trajectory, eventually transitioning from a passing particle orbit to a trapped particle orbit.

The preceding comparison was performed at equal numerical step size to highlight the qualitative distinc-

tions in the trajectories generated by the respective algorithms. Which algorithm proves preferable for a specific application depends on many factors including: the required accuracy, the numerical quantities of interest, the timescales of interest, and the relative computational expense of the two algorithms. Over sufficiently long times, the conservative algorithm will eventually out-perform the non-conservative algorithm, but the timescale for this may be longer than the timescale of interest for particular problems especially under equal computational expense comparisons; the implicit DVI advance is several times more expensive than the explicit RK4 advance on a per-step basis[33], and the error of the RK4 scheme, being fourth-order accurate, decreases rapidly as the step size is reduced. Still, energetic particle processes often require long time integrations, and there is great interest in conservative algorithms for modeling these processes[10,11,28,29,57,62,63].

Note that the conservative character of the DVI does not preclude the incorporation of dissipative dynamics, such as collisional drag. It has been shown how to use a modified statement of the least action principle, known as a Lagrange-d'Alembert principle, to incorporate dissipative effects into the time advance[33], in which case it remains important that all dissipation is due to physical effects rather than an unknown combination of physical and numerical dissipation.

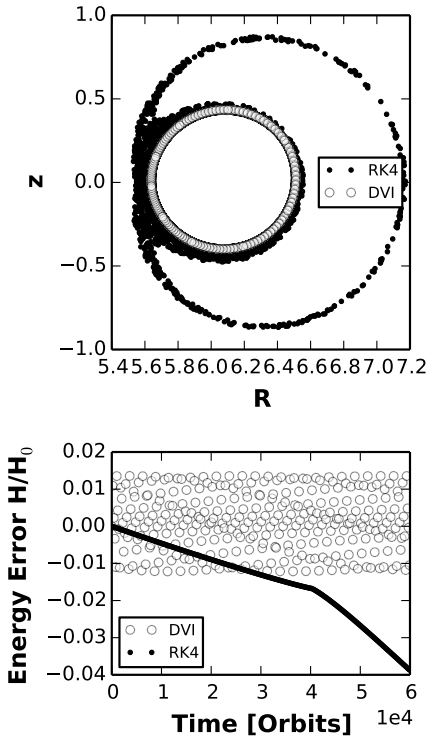

FIG. 6. The DVI exhibits excellent long-term fidelity in the integration of a 3.5 MeV passing alpha-particle orbit. The RK4 advance accumulates global errors in an undesirable way, eventually leading to the transition to a trapped particle banana orbit.

IV. DISCUSSION

In this paper, we have developed a new technique for the symplectic integration of non-canonical Hamiltonian systems based on degenerate variational integrators. We have shown that in order to capture the geometry of the dynamics — including the order of the dynamical system and the area-preserving symplectic flow — it is important that the variational discretization retain the degeneracy of the Lagrangian. Toward this end, we provided a simple means of checking for degeneracy based on a Hessian matrix of second-order derivatives.

For canonical Hamiltonian systems, the DVI technique can be used to derive the familiar Leapfrog advance. For non-canonical applications of interest, the DVI technique enables the first one-step non-canonical symplectic integrators for magnetic field line flow and a class of guiding center trajectories. In both cases, an electromagnetic gauge is chosen to facilitate the degenerate discretization. For guiding center trajectories, an additional assumption about the orientation of the magnetic field is also assumed (an assumption relaxed in a related work[41]). The numerical demonstrations presented here verify the new, non-canonical symplectic integrators capture the qualitative Hamiltonian behavior of the dynamics while eliminating instabilities present in previous guiding center variational integrators.

Prospects for future work persist in both improved plasma physics algorithms and the numerical analysis of DVIs. In terms of plasma physics algorithms, natural progressions of this work include higher-order accuracy and adaptive time stepping. While pursuing higher-order accuracy, the care must be taken to retain the preservation of the non-canonical symplectic structure. Eventually, this particle-advance scheme and its decedents may be used in structure-preserving drift- and gyro-kinetic simulations, analogous to recent work in multisymplectic PIC simulations[12–14,16,64]. In terms of numerical analysis, DVIs introduce interesting considerations such as the non-canonical symplectic structures that converge to the continuous structure in the zero-step size limit. Much of the analysis of canonical symplectic integrators assumes the algorithm preserves the same two-form; it will be valuable and interesting to determine rigorous implications of this more general class of symplectic algorithms. Additionally, it would be important to determine how to construct a properly degenerate variational integrator for the fully general non-canonical phase-space Lagrangian in Eq. (27), thereby providing a solution for the long-standing issue of symplectic integration in non-canonical coordinates.

V. ACKNOWLEDGMENTS

This work was performed under the auspices of the U.S. Department of Energy by Lawrence Livermore National Laboratory under contract DE-AC52-07NA27344; under the auspices of the NNSA of the U. S. DOE by Los Alamos National Laboratory, operated by LANS LLC under DOE contract No. DEAC52-06NA25396; and by the Princeton Plasma Physics Laboratory under contract number DE-AC02-09CH11466. This project has received funding from the European Unions Horizon 2020 research and innovation programme under the Marie Skłodowska-Curie grant agreement No 708124. The authors are grateful to Jonathan Squire, Yao Zhou and Daniel Ruiz for valuable conversations. LLNL-JRNL-744319-DRAFT

[1] R. G. Littlejohn, Journal of Plasma Physics **29**, 111 (1983).
[2] J. R. Cary and R. G. Littlejohn, Annals of Physics **151**, 1 (1983).
[3] J. R. Cary and A. J. Brizard, Reviews of Modern Physics **81**, 693 (2009).
[4] L. D. Landau and E. M. Lifshitz, *Mechanics* (Pergamon Press, 1969).
[5] A. J. Lichtenberg and M. A. Lieberman, *Regular and Stochastic Motion* (Springer Science + Business Media, 1983).
[6] J. E. Marsden and T. S. Ratiu, *Introduction to Mechanics and Symmetry* (Springer Science and Business Media, 1999).
[7] E. Hairer, C. Lubich, and G. Wanner, "Geometric numerical integration," (Springer, 2006) pp. 179–236.
[8] R. I. McLachlan and G. R. W. Quispel, Journal of Physics A: Mathematical and General **39**, 5251 (2006).
[9] E. Forest and R. D. Ruth, Physica D **43**, 105 (1990).
[10] H. Qin and X. Guan, Physical Review Letters **100**, 035006 (2008).
[11] H. Qin, X. Guan, and W. M. Tang, Physics of Plasmas **16**, 042510 (2009).
[12] J. Squire, H. Qin, and W. M. Tang, Physics of Plasmas **19**, 084501 (2012).
[13] E. Evstatiev and B. Shadwick, Journal of Computational Physics **245**, 376 (2013).
[14] B. A. Shadwick, A. B. Stamm, and E. G. Evstatiev, Physics of Plasmas **21**, 055708 (2014), http://dx.doi.org/10.1063/1.4874338.
[15] A. B. Stamm, *Variational formulation of macro-particle algorithms for studying electromagnetic plasmas*, Doctoral Thesis, University of Nebraska - Lincoln (2015), https://digitalcommons.unl.edu/dissertations/AAI3738970.
[16] H. Qin, J. Liu, J. Xiao, R. Zhang, Y. He, Y. Sun, J. Burby, C. Ellison, and Y. Zhou, Nuclear Fusion **56**, 014001 (2016).
[17] G. Darboux, Bulletin des Sciences Mathématiques **6**, 14 (1882).
[18] R. B. White and M. S. Chance, Physics of Fluids **27**, 2455 (1984).
[19] R. White and L. E. Zakharov, Physics of Plasmas **10**, 573 (2003).
[20] S. Zhang, Y. Jia, and Q. Sun, Journal of Computational Physics **282**, 43 (2014).
[21] B. Karasözen, Mathematical and Computer Modelling **40**, 1225 (2004).
[22] Note that methods have been developed for Lie-Poisson systems[? ?] ; however, the magnetic field line and guiding center Poisson brackets are not Lie-Poisson brackets.
[23] J. L. Velasco, A. Bustos, F. Castejon, L. A. Fernandez, V. Martin-Mayor, and A. Tarancon, Computer Physics Communications **183**, 1877 (2012).
[24] G. J. Kramer, R. V. Budny, A. Bortolon, E. D. Fredrickson, G. Y. Fu, W. W. Heidbrink, R. Nazikian, E. Valeo, and M. A. V. Zeeland, Plasma Physics and Controlled Fusion **55**, 025013 (2013).
[25] D. Pfefferlé, J. P. Graves, W. A. Cooper, C. Misev, I. T. Chapman, and M. T. ans S Sangaroon, Nuclear Fusion **54**, 064020 (2014).
[26] E. Hirvijoki, O. Asunta, T. Koskela, T. Kurki-Suonio, J. Meittunen, S. Sipilä, A. Snicker, and S. Äkäslompolo, Computational Physics Communications **185**, 1310 (2014).
[27] E. Hirvijoki, T. Kurki-Suonio, S. Äkäslompolo, J. Varje, T. Koskela, and J. Meittunen, Journal of Plasma Physics **81**, 435810301 (2015).
[28] J. Li, H. Qin, Z. Pu, L. Xie, and S. Fu, Physics of Plasmas **18**, 052902 (2011).
[29] M. Kraus, *Variational Integrators in Plasma Physics*, Doctoral Thesis, Technische Universität München (2013).
[30] J. E. Marsden and M. West, Acta Numerica **10**, 357514 (2001).
[31] J. Squire, H. Qin, and W. M. Tang, Physics of Plasmas **19**, 052501 (2012).
[32] C. L. Ellison, J. M. Finn, H. Qin, and W. M. Tang, Plasma Physics and Controlled Fusion **57**, 054007 (2015).
[33] C. L. Ellison, *Development of Multistep and Degenerate Variational Integrators for Applications in Plasma Physics*, Doctoral Thesis, Princeton University (2016).
[34] F. Bashforth and J. C. Adams, *An attempt to test the theories of capillary action by comparing the theoretical and measured forms of drops of fluid, with an explanation of the method of integration employed in constructing the tables which give the theoretical forms of such drops* (Cambridge University Press, 1883).
[35] G. Dahlquist, Mathematica Scandinavica **4**, 33 (1956).
[36] E. Hairer, C. Lubich, and G. Wanner, "Geometric numerical integration," (Springer, 2006) pp. 567–616.
[37] H. Goldstein, C. Poole, and J. Safko, *Classical Mechanics* (Addison Wesley, 2001).
[38] C. W. Rowley and J. E. Marsden, Proceedings of the 41st IEEE Conference on Decision and Control **2**, 1521 (2002).
[39] S. Ober-Blöbaum, M. Tao, M. Cheng, H. Owhadi, and J. E. Marsden, Journal of Computational Physics (2013).
[40] T. Tyranowski and M. Desbrun, arXiv:1401.7904 (2014).
[41] J. W. Burby and C. L. Ellison, Physics of Plasmas **24**, 110703 (2017), https://doi.org/10.1063/1.5004429.
[42] M. Kraus, "Projected variational integrators for degenerate lagrangian systems," (2017), arXiv:1708.07356 [math.NA].
[43] R. D. Ruth, IEEE Transactions on Nuclear Science **NS-30**, 2669 (1983).
[44] P. J. Channell and C. Scovel, Nonlinearity **3**, 231 (1990).
[45] J. M. Sanz-Serna, BIT **28**, 877 (1988).
[46] M. Leok and J. Zhang, IMA Journal of Numerical Analysis **31**, 1497 (2011).
[47] V. I. Arnold, *Mathematical Methods of Classical Mechanics* (Springer, 1989) p. 243.
[48] H. Goldstein, C. Poole, and J. Safko, *Classical Mechanics* (Addison Wesley, 2001) Chap. 8.5, p. 353.
[49] The fixed endpoint condition introduces technical nuance on the existence of a path connecting such endpoints, especially for phase-space and degenerate Lagrangians. See e.g. Ref. 40 for technical details.
[50] Fermat's principle provides one interesting example of a degenerate Lagrangian that is not a phase-space Lagrangian: $L = n(x,y)\sqrt{\dot{x}^2 + \dot{y}^2}dt$, where n is the index of refraction and we have set $c = 1$. This is a special case of geodesics.
[51] D. D. Holm, T. Schmah, and C. Stoica, *Geometric Mechanics and Symmetry: From Finite to Infinite Dimensions* (Oxford University Press, 2009).
[52] T. Frankel, *The Geometry of Physics: An Introduction*, 3rd ed. (Cambridge University Press, 2012).
[53] E. Hairer, Numerische Mathematik **84**, 199 (1999).
[54] E. Hairer, C. Lubich, and G. Wanner, "Geometric numerical integration," (Springer, 2006) pp. 3–4.
[55] E. Hairer, C. Lubich, and G. Wanner, "Geometric numerical integration," (Springer, 2006) p. 42.
[56] S. Blanes, F. Casas, and A. Murua, SIAM Journal on Numerical Analysis **42**, 531 (2004).
[57] Y. He, Y. Sun, R. Zhang, Y. Wang, J. Liu, and H. Qin, Physics of Plasmas **23**, 092109 (2016).
[58] T. G. Northrop, Reviews of Geophysics **1**, 283 (1963).

[59]H. Yoshida, Physics Letters A **150**, 262 (1990).
[60]A. Friedman and S. P. Auerbach, Journal of Computational Physics **93**, 171 (1991).
[61]Recall that B is normalized by e/mc, so this field is not 255.6 T.
[62]Y. He, Y. Sun, J. Liu, and H. Qin, Journal of Computational Physics **281**, 135 (2015).
[63]Y. Wang, J. Liu, H. Qin, Z. Yu, and Y. Yao, Computer Physics Communications **220**, 212 (2017).
[64]M. Kraus, K. Kormann, P. Morrison, and E. Sonnendrcker, Journal of Plasma Physics **83** (2017), 10.1017/S002237781700040X.